REPORT DOCUMENTATION PAGE

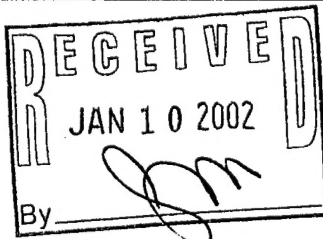Form Approved
OMB NO. 0704-0188

Public Reporting burden for this collection of information is estimated to average 1 hour per response, including the time for reviewing instructions, searching existing data sources, gathering and maintaining the data needed, and completing and reviewing the collection of information. Send comment regarding this burden estimates or any other aspect of this collection of information, including suggestions for reducing this burden, to Washington Headquarters Services, Directorate for information Operations and Reports, 1215 Jefferson Davis Highway, Suite 1204, Arlington, VA 22202-4302, and to the Office of Management and Budget, Paperwork Reduction Project (0704-0188,) Washington, DC 20503.

1. AGENCY USE ONLY (Leave Blank)	2. REPORT DATE 4-30-01	3. REPORT TYPE AND DATES COVERED 8-8-96 to 7-31-99

4. TITLE AND SUBTITLE	5. FUNDING NUMBERS
3-D CRYO-COOLED MULTI-CHIP MODULES VIA OPTICAL INTERCONNECTS	DAAD04-96-1-0324 DAAH04-96-1-0324

6. AUTHOR(S)
Len Schaper

7. PERFORMING ORGANIZATION NAME(S) AND ADDRESS(ES) University of Arkansas Electrical Engineering Fayetteville, AR. 72701	8. PERFORMING ORGANIZATION REPORT NUMBER

9. SPONSORING / MONITORING AGENCY NAME(S) AND ADDRESS(ES) U. S. Army Research Office P.O. Box 12211 Research Triangle Park, NC 27709-2211	10. SPONSORING / MONITORING AGENCY REPORT NUMBER 36199.1 - RT-DPS

11. SUPPLEMENTARY NOTES
The views, opinions and/or findings contained in this report are those of the author(s) and should not be construed as an official Department of the Army position, policy or decision, unless so designated by other documentation.

12 a. DISTRIBUTION / AVAILABILITY STATEMENT Approved for public release; distribution unlimited.	12 b. DISTRIBUTION CODE

13. ABSTRACT (Maximum 200 words)

We have investigated, both theoretically and experimentally, the formation of optical waveguides as optical interconnects in the semiconductor InP. A dark soliton was also investigated and demonstrated to also act as a waveguide and guide a second beam. These waveguides and their interaction offer exciting possibilities for use as optical interconnects in multi-chip modules.

14. SUBJECT TERMS		15. NUMBER OF PAGES 10
		16. PRICE CODE

17. SECURITY CLASSIFICATION OR REPORT UNCLASSIFIED	18. SECURITY CLASSIFICATION ON THIS PAGE UNCLASSIFIED	19. SECURITY CLASSIFICATION OF ABSTRACT UNCLASSIFIED	20. LIMITATION OF ABSTRACT UL

NSN 7540-01-280-5500

Standard Form 298 (Rev.2-89)
Prescribed by ANSI Std. 239-18
298-102

20020125 268

RECEIVED
JAN 10 2002
By

MEMORANDUM OF TRANSMITTAL

TO: U.S. Army Research Office
      ATTN: AMSRL-RO-BI (TR)
      P.O. Box 12211
      Research Triangle Park, NC 27709-2211

FROM: Professor Len Schaper
      Director of HiDEC
      University of Arkansas
      Electrical Engineering
      Fayetteville, AR 72701

DOD REPORT ON 3-D CRYO-COOLED MULTI-CHIP MODULES
VIA OPTICAL INTERCONNECTS
DAAH04-96-1-0324
AUGUST 8, 1996 TO JULY 31, 1999

ABSTRACT

We have investigated, both theoretically and experimentally, the formation of optical waveguides as optical interconnects in the semiconductor InP. A dark soliton was also investigated and demonstrated to also act as a waveguide and guide a second beam. These waveguides and their interaction offer exciting possibilities for use as optical interconnects in multi-chip modules.

FINAL REPORT

DOD REPORT ON 3-D CRYO-COOLED MULTI-CHIP MODULES VIA OPTICAL INTERCONNECTS

DAAH04-96-1-0324

AUGUST 8, 1996 TO JULY 31, 1999

Self-trapping of beams in photorefractive semiconductors offers several attractive features when compared with more conventional materials such as strontium barium niobate. For example, operation at optical telecommunications wavelengths and fast response times combined with very low operation power levels are a few of the advantages offered. These properties can lead to many exciting applications, such as, reconfigurable switches, interconnects, and self-induced waveguide devices. Unfortunately, photorefractive semiconductors tend to have tiny electro-optic coefficients, which imply that a "conventional" screening soliton in such materials would require applied fields that are too large for most applications. But Fe-doped photorefractive InP crystals displays photorefractive effects that stem from excitation of both electrons and holes, and, when the photo-excitation rate of holes is comparable with the thermal excitation rate of electrons, the induced space charge field is resonantly-enhanced by more than an order of magnitude. That is, the internal photo-induced field exceeds 50 kV/cm even when the applied (bias) field is 5 kV/cm or less. This enhancement appears only at the vicinity of a particular intensity of the beam. Furthermore, if a given polarity of the applied field leads to self-focusing at intensities below the resonant intensity, the same polarity leads to beam breakup and defocusing when the intensity exceeds the resonant intensity. These features are truly unique to photorefractive solitons in InP and cannot be explained by the established theory of photorefractive screening solitons. In
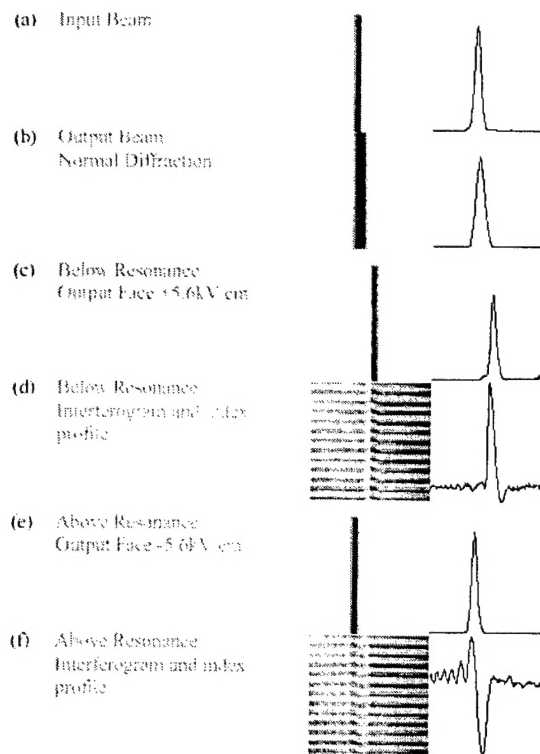

(a) Input Beam

(b) Output Beam
Normal Diffraction

(c) Below Resonance
Output Face +5.6kV/cm

(d) Below Resonance
Interferogram and index profile

(e) Above Resonance
Output Face -5.6kV/cm

(f) Above Resonance
Interferogram and index profile

Fig. 1. One-dimensional interconnects in InP

1

fact, all the theories describing all soliton effects in photorefractive do not show any resonance of any sort.

A photorefractive soliton[1-9] is created when a photo-induced index change exactly compensates for the diffraction of the beam. In this sense the beam is able to create its own waveguide and offers potential for applications in the field of all-optical switching and beam steering. These effects have been extensively studied in ferroelectric oxide and sillenite oxide crystals for visible wavelengths. For the near infra-red wavelengths used in telecommunications, InP:Fe crystals have already demonstrated interesting photorefractive properties[10-13] and self-trapping of a one-dimensional beam had been reported by our research group (fig.1).[14] In the research supported by this grant we report on the first observation of trapping of a two-dimensional Gaussian beam at 1.3μm, guiding of a second beam at the telecommunications wavelength 1.55μm and on the results from collisions between two spatial solitons.

EXPERIMENTAL RESULTS

For the experiment on 2-D waveguide formation the beam from a Nd:Yag laser at 1.3μm is collimated and focused with a 5cm focal length lens on the entrance face of an InP:Fe crystal whose temperature is stabilized at 297K. The electric field, E_0, is applied along <110>, while the beam propagates along <1$\bar{1}$0>, and is polarized either horizontally or vertically at 45° from <110>.

Figure 2 shows an example of 2-D trapping using this configuration. The beam size at the entrance face of the crystal has a diameter of about 55μm and diverges to a 170μm diameter at the exit face when no field is applied to the crystal. The InP:Fe crystal length is 1cm in the direction of the propagation. When a 12 kV/cm field is applied to the crystal, the beam is trapped and the beam diameter at the exit face is elliptical and reduced to about 55μm by 65 μm. Our experiments show that for exactly the same value of all parameters,
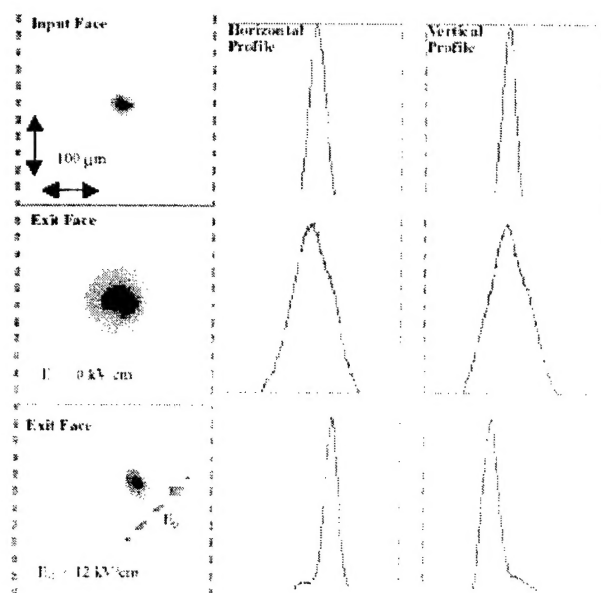

Fig. 2. Two-dimensional interconnect formation in InP

the beam is trapped to the same diameter for either a 1cm or a 0.5cm crystal length, supporting the conclusion that the trapped diameter is the same throughout the crystal. To show that an

efficient waveguide is formed in the crystal, we have also propagated a 1.55μm ($\cong$ 1mW/cm^2) laser beam collinear to the 1.3μm(1W/cm^2) trapped laser beam. To observe only the 1.55μm beam, a color filter is placed after the crystal. When both beams are present and vertically polarized, the 1.55μm beam is observed to be guided along the same direction as the 1.3μm beam. However, when the polarization of the 1.3μm beam is changed to horizontal and the 1.55μm beam kept vertical, the 1.55μm beam is guided on the side of the 1.3μm trapped beam. While in both cases the 1.55μm beam is guided, we can see that when the two beams have orthogonal polarizations, the 1.55μm beam is more efficiently guided and has a near circular profile. The background noise is at least an order of magnitude below the trapped beam.

In order to measure the index change responsible for this large focusing effect, an interferometer is added to the apparatus (Fig. 1). Specifically, a 1.3μm wavelength probe beam is launched through the crystal to monitor the refractive index. The probe beam is an expanded beam polarized perpendicularly to the focused beam. It is also lower in intensity than the focused beam, so that it does not perturb the photorefractive space-charge field. With this orientation an index change with the same magnitude, but with opposite signs, is seen by the two beams. A rotatable polarizer, positioned after the crystal, selectively isolated either beam for imaging onto the camera. When the probe beam is imaged on the camera, a reference beam which is identically polarized is also present. In this way an interference pattern depicting the index change in the InP:Fe crystal is obtained.

To evaluate the character of the photorefractive index change occurring in our experiment the electro-optic coefficient, r_{41}, is first determined by measuring the fringe shift with application of an applied field without the focused self-trapped beam present. The fringes shift one quarter of a fringe when the applied field E_0 is switched from 5.4kV/cm to -5.4kV/cm. This measurement gives a refractive index change equal to 2.5 10^{-5} and corresponds to an electro-optic coefficient, r_{41} = -1.42 10^{-12}pm/V, which is in accordance with the literature.[15] In fig.1 the fringe contours, with and without the focused self-trapped beam present are shown we can see that the focusing or waveguiding effect is induced by an increase of the refractive index in the center of the beam while a strong decrease (10^{-4}) of the index appears on one side of the beam. This amazingly strong decrease of the index implies that a large photorefractive space charge field is present. We calculate this space charge field to be about 50kV/cm when the applied field is only E_0 = 5kV/cm. Despite the small value of the electro-optic coefficient r_{41}, it is clearly possible to induce large index changes. Physically, the large index change is due to the large space charge field that can be created because of both the intensity temperature resonance and the low value of the dielectric constant associated with InP.

THEORETICAL RESULTS

In our work we developed the first model describing the resonant self-focusing effects in photorefractive semiconductors. The theory is based on a model that relies on two-donor levels, one deep trap level and conduction of both electrons and holes. That model, although successful in explaining two-wave-mixing, cannot explain self-focusing effects, because it relies on a single periodic interference grating at low visibility (modulation depth). Even a superposition of such gratings cannot be applied to explain self-focusing of localized beams. Yet, the underlying assumptions about the rate equations hold for a localized beam and serve as a starting point for our theory.

We start with the standard set of equations in temporal steady state: the continuity equations for electrons and holes respectively, the rate equation for deep traps level, the transport equation and Gauss law.

$$e_n n_t - \gamma_n n p_t + \frac{dJ_n}{dx} = 0 \qquad (1a)$$

$$e_p p_t - \gamma_p p n_t + \frac{dJ_p}{dx} = 0 \qquad (1b)$$

$$-e_n n_t + \gamma_n n p_t + e_p p_t - \gamma_p p n_t = 0 \qquad (1c)$$

$$J_n = q n \mu_n E + q D_n \frac{dn}{dx} \qquad (1d)$$

$$J_p = q p \mu_p E - q D_p \frac{dp}{dx} \qquad (1e)$$

$$\frac{dE}{dx} = \frac{e}{\varepsilon}[Nd - Na + p - n - n_t] \qquad (1f)$$

where $e_n = e_n^{th} + \phi_n I(x)$ and $e_p = e_p^{th} + \phi_p I(x)$. e_n^{th} and e_p^{th} are the thermal emission rates. ϕ_n and ϕ_p are the photoionization cross sections, ϕ_n and ϕ_p are the photoionization cross sections, I is the optical intensity and Nd, Na are the donors and acceptors concentrations. n_t and p_t are the concentration of filled and ionized traps respectively. We seek an expression for the space charge field as a function of the optical intensity, I, for a single optical beam whose width is much larger than the optical wavelength. In such cases, the diffusion currents are negligible. Furthermore, for typical value of the parameters, the optical excitation of electrons, as well as the thermal excitation of holes can be neglected. It is possible to show (analytically) that, within a very good approximation, the electron concentration is proportional to the holes concentration. The physical meaning of this finding is that the electron and hole currents are both constants, not

only their sum. Keeping in mind that diffusion currents are neglected, one can easily see why
p(x)=constant n(x) (where the constant is a positive number calculated at the boundary of the
crystal). Using this relation in Eq.(1c) and substituting (1d) in (1c), we obtain

$$E(x) = E_0 \frac{I_{res}(x) - I_b}{I_{res}(x) - I(x)} \qquad (2)$$

Where $I_{res}(x) = e_n \, n_t(x)/(\phi_p \, p_t(x))$ is the local resonance intensity. In the same manner that
$\phi_p \, p_t I$ is the rate of trap filling, $\phi_p \, p_t \, I_{res}$ is the rate of thermal ionization.
Therefore $I_{res}(x) - I(x)$ is proportional to the net ionization rate of the trap level. In steady state,
this rate must be compensated by the net recombination rate, which is given by the numerator of
(2) times the electrons (or holes) concentration. Note that, through Gauss law, I_{res} is a function
of the derivative of the electric field (the free carriers density in Gauss law can be neglected). If
dE/dx is small enough, I_{res} is roughly constant, and thus the space charge field can be written as

$$E(x) = E_0 \frac{I_{res0} - I_b}{I_{res0} - I(x)} \quad , \qquad (3)$$

where $I_{res0} = e_n \, n_{t0}/(\phi_p \, p_{t0})$ and $n_{t0} = Nd - Na$. Clearly, the space charge field exhibits
resonance effects when $I = I_{res0}$. This expression is no longer valid at the resonance, yet
numerical solutions of (2) show that it is valid up to $I_{max} = 0.8 I_{res0}$, where I_{max} is the peak
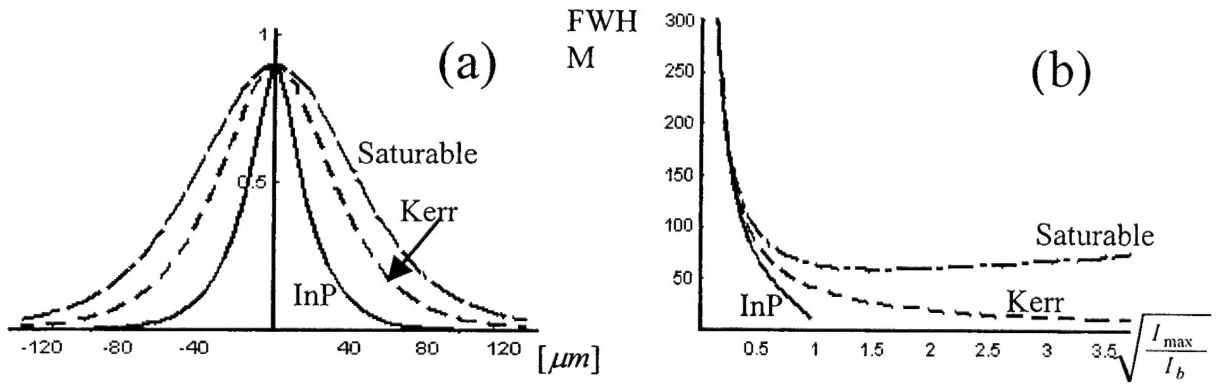

Fig 3: Soliton wavefunctions (a) and existence curves (b) for kerr ($\Delta n \propto I$), saturable ($\Delta n \propto I/(1+I)$)

and InP ($\Delta n \propto 1/(1-I)$) nonlinearities.

intensity of the beam. From $E(x)$ of Eq. (3) one can find the nonlinear change in the refractive index, $\Delta n(x) \propto E(x)$, substitute it in the nonlinear wave equation describing beam propagation,[3,4] and seek stationary solutions, that is, spatial solitons. Using techniques similar to those of Refs. 3,4, we obtain the solitons wavefunctions and the soliton existence curve shown in Fig. 1.

The wavefunction of a soliton at $I_{max} = 0.8 I_{res0}$ is shown in Fig 1a. For comparison, we also show the respective soliton wavefunctions for the Kerr and the saturable nonlinearities. In Fig 1b we show the existence curve of each nonlinearity. As shown Fig. 1a, the normalized width of the resonant (InP) soliton is considerably narrower than that of the Kerr and the saturable nonlinearities, implying that solitons of the same width require a lower change in $\Delta n(x)$ for the resonant solitons (a factor of 2 at $I_{max} = 0.8 I_{res0}$). This is why photorefractive solitons in InP can be observed in spite of the fact that the electrooptic coefficient of InP is more than 100 times smaller than that of SBN. Furthermore, the resonant nonlinearity of solitons in InP does **not** saturate (as the nonlinearity of all screening solitons does), but rather deforms. As the light intensity increases, the waveguide becomes more and more asymmetric. This asymmetry stems from the electric field derivative in (1f), which is no longer negligible. In Fig 2 we can see a numerical solution for $I_{max} = 1.3 I_{res0}$.
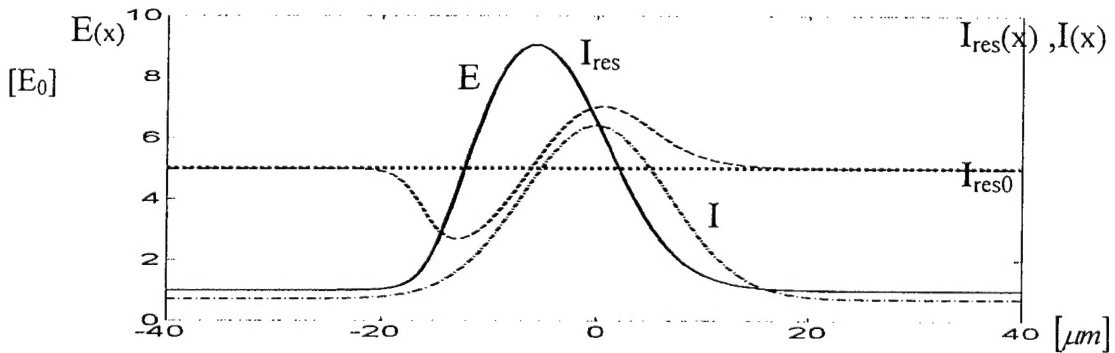

Fig 4: The space charge field $E(x)$, (solid curve) and local resonant intensity $I_{res}(x)$ (dashed) for a given optical intensity distribution $I(x)$ (dash dotted). Note that at the peak, $I < I_{res} = I_{res0}$.

The resonance intensity is modified by the field derivative in such a way that the peak of the field is being shifted from the center. It is interesting to note that at extremum points ($E'=0$) expression (2) still holds. This leads to important conclusion: Since the numerator of (2) is positive and the field maximum is also positive, then the numerator must be positive as well. In other words the maximum value of the electric field will take place at a point for which $I(x) < I_{res0}$. This explains why for $I_{max} >> I_{res0}$ the beam undergoes linear diffraction[1]: the induced waveguide and the beam no longer overlap. These results compare well with Fig.1.

While our theory has been strong we have also carried out experiments that demonstrate that photorefractive spatial solitons can be formed in semi-insulating InP:Fe[1,2] through the formation of self-induced waveguides. Our most recent work, however, carried out under support of this grant, is on the coherent collision between two solitons in InP at the telecommunications wavelength of 1.3 μm to form a y-junction.

For the experiment, light from a diode laser is split into two beams. Lenses are used to independently focus each of the beams onto the crystal's entrance face when observing the collision between two-dimensional solitons, while spherical lenses are used to observe the collision between two-dimensional solitons. The light is polarized vertically, along the <110> crystal axis, while the electric field is applied horizontally along the <001> axis. The beams are arranged so that they are parallel in the horizontal plane. The relative phase between the two beams is controlled through the use of a piezoelectric mirror in the one beam.

Before observing a collision in InP, each beam is checked independently to verify that it forms a soliton. Both beams are then launched together and the collision between one-dimensional solitons is observed (Fig 5). Fig. 2a shows the input of the individual beams while Fig. 2b shows the normally diffracted output of each beam. With an applied field of negative 11.5 kV, the output diameter of each separately is reduced (Fig. 2c). The collision of the two solitons, when the beams are in phase (Fig. 2d), results in a single peak with a width of 23 μm that is located centrally between the locations of the individual solitons. We found similar results with a 180-degree phase difference but in this case the two beam defected each other. Finally we also investigate and demonstrated the formation of a dark soliton in InP. We used the dark notch formed to guide a second laser beam (Fig. 6).

(a) Entrance Face
     25 μm width
     20 μm separation

(b) Exit Face
     Normal Diffraction
     46 μm width

(c) Exit Face
     Individual Solitons
     25 μm width

(d) Exit Face
     Merged Solitons
     27 μm

Fig. 5 Collision between two in phase solitons in InP

In summary, we have explained how a mechanism based on conduction of both (thermal) electrons and (photo-excited) holes leads to a resonant enhancement (by more than an order of magnitude) of the space charge field. This enhancement is crucial to the observation of
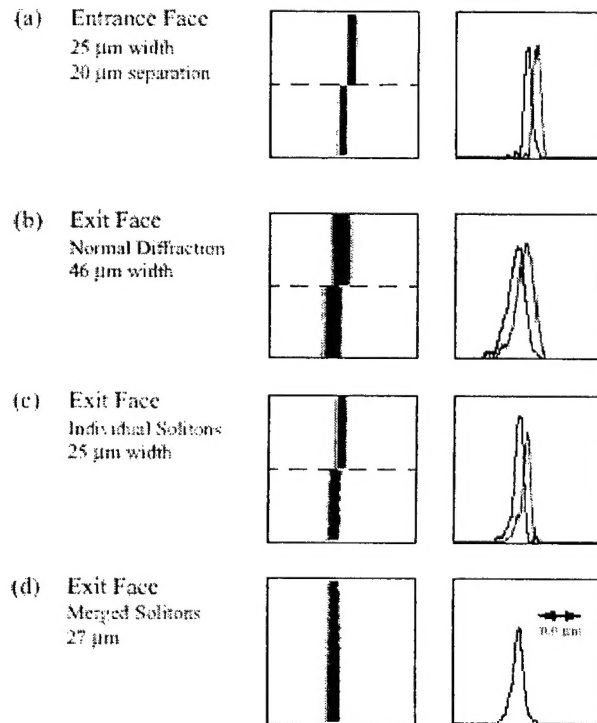
solitons in semiconductors photorefractive semiconductors described below. An analytical expression for the field in the sub-resonance regime was derived, and the characteristics of solitons (wavefunctions, existence curve) were calculated. Other observed effects such as soliton collisons could be explained on the same basis. Experimentally, we have investigated the collision between solitons and found that the interaction between solitons is dependent upon the relative phase between the two beams. For a collision between two solitons with the beams in-phase, the solitons merge to form a y-junction. When the two beams are out of phase, the two solitons deflect each other. We also demonstated a dark soliton and its ability to act as a waveguide.
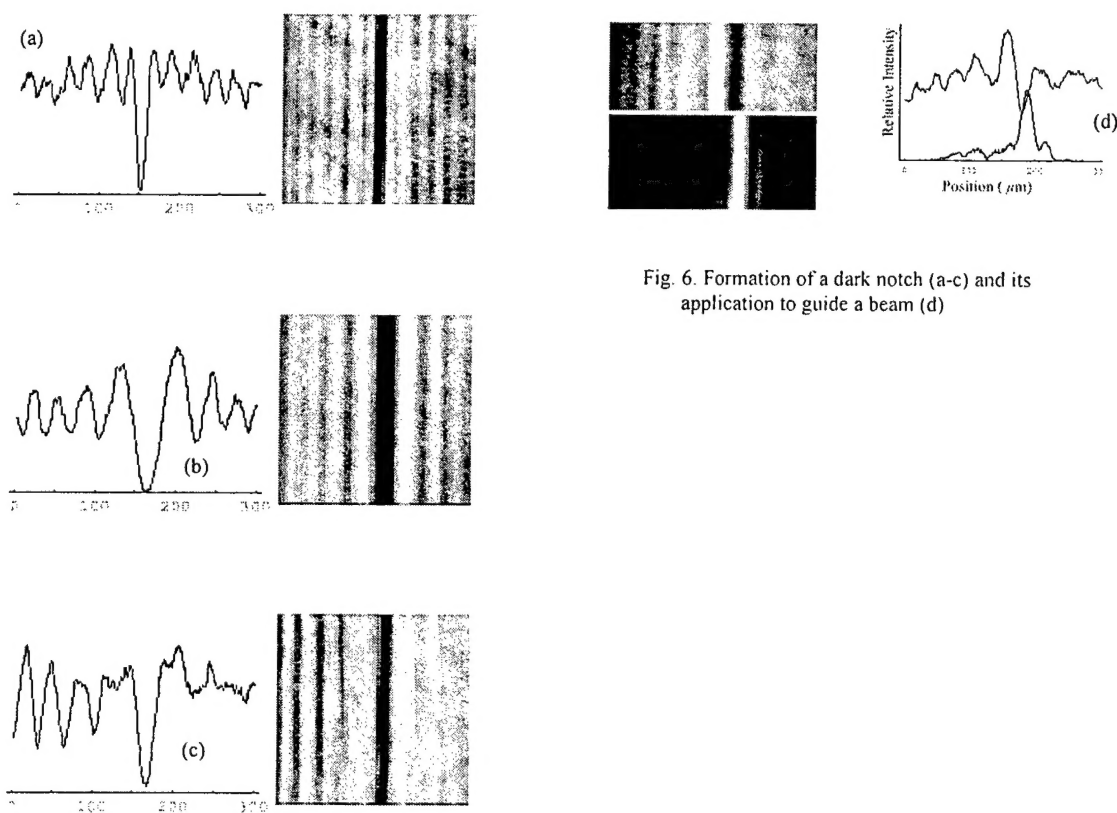

Fig. 6. Formation of a dark notch (a-c) and its application to guide a beam (d)

MANUSCRIPTS

1. Two-dimensional Self-trapping and Guiding in InP, M. Chauvet, S. A. Hawkins, D. Bliss, M. Segev, G. J. Salamo, **Appl. Phy. Lett.**, **70,** 2499, 1997

PARTICPANTS

Mr. Scot Hawkins received his Ph.D. degree at the University of Arkansas at the end of the fall semester of 1999 as a result of support by this grant.

INVENTIONS

We have not reported or claim any inventions.

TECHNOLOGY TRANSFER

Although we have not established a transfer of technology at the project completion, we are still pursuing the possibility.